

663173
DP-1417

21

TIS FILE
RECORD COPY

DENITRATION OF SAVANNAH RIVER PLANT WASTE STREAMS

E. G. OREBAUGH



SAVANNAH RIVER LABORATORY
AIKEN, SOUTH CAROLINA 29801

PREPARED FOR THE U.S. ENERGY RESEARCH AND DEVELOPMENT ADMINISTRATION UNDER CONTRACT AT(07-2) 1

NOTICE

This report was prepared as an account of work sponsored by the United States Government. Neither the United States nor the United States Energy Research and Development Administration, nor any of their contractors, subcontractors, or their employees, makes any warranty, express or implied, or assumes any legal liability or responsibility for the accuracy, completeness or usefulness of any information, apparatus, product or process disclosed, or represents that its use would not infringe privately owned rights.

Printed in the United States of America

**Available from
National Technical Information Service
U. S. Department of Commerce
5285 Port Royal Road
Springfield, Virginia 22161**

Price: Printed Copy \$4.00; Microfiche \$2.25

063173

DP-1417

Distribution Category: UC-10

DENITRATION OF SAVANNAH RIVER PLANT WASTE STREAMS

by

E. G. Orebaugh

Approved by

M. L. Hyder, Research Manager
Separations Chemistry Division

Publication Date: July 1976

**E. I. DU PONT DE NEMOURS AND COMPANY
SAVANNAH RIVER LABORATORY
AIKEN, SOUTH CAROLINA 29801**

PREPARED FOR THE U. S. ENERGY RESEARCH AND DEVELOPMENT ADMINISTRATION UNDER CONTRACT AT(07-2)-1

ABSTRACT

Partial denitration of waste streams from Savannah River Plant separations processes was shown to significantly reduce the quantity of waste solids to be stored as an alkaline salt cake. The chemical processes involved in the denitration of nonradioactive simulated waste solutions were studied. Chemical and instrumental analytical techniques were used to define both the equilibrium concentrations and the variation of reactants and products in the denitration reaction. Mechanisms were proposed that account for the complicated chemical reactions observed in the simulated waste solutions.

Metal nitrates can be denitrated by reaction with formic acid only by the release of nitric acid from hydrolysis or formate complexation of metal cations. However, eventual radiolysis of formate salts or complexes results in the formation of bicarbonate and makes complexation-denitration a nonproductive means of reducing waste solids. Nevertheless, destruction of nitrate associated with free acid and easily hydrolyzable cations such as iron, mercury, and zirconium can result in >30% reduction in waste solids from five SRP waste streams.

CONTENTS

Introduction	5
Background	6
Experimental Procedure	7
Chemical Analysis	7
Gas Analysis	8
Denitration Tests	8
Results	9
Nitration-GSWS Denitrations	9
Sulfate-GSWS Denitrations	16
Denitration of Simulated Purex LAW	21
Reaction Mechanisms	22
References	26

DENITRATION OF SAVANNAH RIVER PLANT WASTE STREAMS

INTRODUCTION

Partial denitration of liquid waste from Savannah River Plant (SRP) separations processes has been proposed as a means of reducing the quantity of salt cake requiring tank storage. This report describes the denitration process, presents experimental data, and estimates the extent of waste volume reduction achievable by denitration.

The feasibility of formic acid denitration has been determined for the five major SRP waste streams (Table 1). The major components of these streams are HNO_3 , $\text{Fe}_2(\text{SO}_4)_3$, $\text{Al}(\text{NO}_3)_3$, and NaNO_3 . Generalized synthetic waste solutions (GSWS) (Table 2) were prepared for denitration studies. The composition of the nitrate-GSWS was chosen so that each cation contributed approximately the same amount of nitrate. The composition of the sulfate-GSWS was chosen so that the iron-to-sulfate ratio was 0.5.

TABLE 1

Nominal Composition of SRP Waste Streams
After Evaporation and Acid Stripping^a

Component	<i>Composition, mol/l</i> <i>Modified Purex (HM Process)^b</i>		<i>Purex Process^b</i>		<i>Neptunium Recovery Processes</i>
	<i>HAW</i>	<i>LAW</i>	<i>HAW</i>	<i>LAW</i>	
H^+	1.75	4.2	1.75	1.78	1.5
Na^+	0	0.303	0.58	1.53	2.15
Fe^{3+}	0.03	0.303	0.101	0.51	0.162
Al^{3+}	2.06	0	0.66	0	0.33
Hg^{2+}	0.022	0	0	0	0
K^+	0	0	0	0	0.116
Mn^{2+}	0	0	0	0	0.116
SO_4^{2-}	0.06	0.606	0.202	1.06	0.32
NO_3^-	7.94	4.2	4.21	2.62	4.81

a. Fission products and actinides are not included.

b. HAW, high-activity waste; LAW, low-activity waste.

TABLE 2

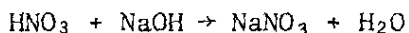
Composition of Generalized Synthetic Waste Solutions (GSWS)

<i>Nitrate-GSWS</i>	<i>Sulfate-GSWS</i>
0.7M HNO ₃	0.70M NaHSO ₄
0.35M Fe(NO ₃) ₃	0.35M Fe(NO ₃) ₃
0.35M Al(NO ₃) ₃	0.35M Al(NO ₃) ₃
1.00M NaNO ₃	0.30M NaNO ₃

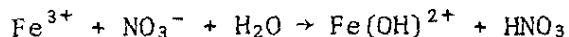
BACKGROUND

Denitration with various organic reductants such as sugars,¹ formaldehyde,^{2,3} paraformaldehyde,⁴ and formic acid^{3,5} has been studied as a means of acid adjustment. Earlier work⁵ demonstrated the controlled destruction of nitric acid to ~1M by the addition of the appropriate quantity of formic acid. Recent work⁶ at Karlsruhe, Germany, has demonstrated formic acid denitration as a means of conditioning a Purex-type waste for a vitrification process.

This study attempted to define denitration conditions that would result in a minimum of waste solids following neutralization with NaOH. Destruction of the nitric acid component of a waste stream eliminates the equivalent amount of NaNO₃ requiring storage by eliminating the reaction



Denitration in the presence of readily hydrolyzable ions also reduces the amount of NaNO₃ ultimately formed by driving reactions such as:



The German work⁶ indicated that by the combined action of hydrolysis and denitration, the denitrated solutions contained only nitrates associated with nonhydrolyzable alkali and alkaline earth metals. The German denitrations reportedly attained an ultimate pH of ~8, which probably resulted from their technique of adding nitrate solution into hot formic acid (reverse strike technique). The formation of formate salts was of no consequence in their following vitrification.

Earlier studies by Healy⁴ showed that the rate of the nitric acid - formic acid reaction was governed by the concentration of nitric acid above 2M. However, the reaction rate constants do not apply at lower acidities because of a change in reaction mechanism. Although rate constants were not developed in this study, the reaction rate became insignificant at acidities less than pH 2 and thus could not be driven by the ionization of formic acid. This fact conflicts with the reported final pH of 8 reported by German⁶ workers.

At the required acidity, only a few easily hydrolyzable cations, such as iron, zirconium, rhodium, silver, and mercury, can be denitrated to oxides and/or hydroxides. Healy⁴ reported that cations not precipitated at pH 3 in aqueous solutions are not precipitated by denitration with formaldehyde. Because the formaldehyde reduction involves formic acid as an intermediate, the statement probably is also valid for the formic acid denitration.

EXPERIMENTAL PROCEDURE

The experimental apparatus was designed to allow volumetric gas measurements, to avoid secondary reactions with air, and to limit evaporative losses over extended reflux periods. The volumetric gas measurements indicated the reaction rate. However, due to the solubility of nitrogen oxide reaction products in both organic (kerosene) and aqueous media in the Wet Test Meter, only the evolved carbon dioxide was actually measured. The reflux condenser ensured that negligible formic acid and water vapor escaped the reaction zone. No volume corrections were applied to the experimental data because the equilibrium volume was within 2% of the original nitrate solution volume.

In the experimental procedure, 50 ml of GSWS in the reaction vessel was heated to a steady boilup rate under a slow purge of inert gas. After a total purge of 3 to 4 system volumes, the purge was disconnected, and the system was allowed to equilibrate under steady reflux. Concentrated formic acid (~24M) was then added in the desired quantity, and the reaction was allowed to proceed under reflux for 4 to 6 hours with hourly sampling of the reaction solution.

Chemical Analysis

All samples of the reaction solution were analyzed for formate, nitrate, and equivalent acidity. The pH and soluble iron concentrations were also determined as supporting data in some experiments. Formate analysis was based on the oxidation of formate to CO₂ with permanganate. However, because both ferric ion

and nitrite interfere, these species were destroyed or removed. Nitrite was destroyed by addition of sulfamic acid; the ferric ion was precipitated by addition of excess sodium carbonate. The alkaline solution was then heated, a measured quantity of permanganate was added, and the solution was boiled for five minutes. Excess permanganate was determined by standard iodometric titration with thiosulfate.

Nitrate analysis was based on a standard addition-potentiometric technique employing an Orion nitrate electrode. Although this electrode responds to nitrite, the nitrate-to-nitrite ratio was sufficiently large in this study to preclude corrections. In the standard addition technique, the change in EMF upon adding a known amount of nitrate to an unknown concentration of nitrate and the decade response (EMF) of the electrode are used in a Nernstian equation to estimate the unknown nitrate concentration.

Equivalent acidity was determined by diluting a 1 ml sample to 20 ml in water and titrating to pH 12. The apparent acid equivalence measured in this way was in error because of dilution of the sample with water and caustic. By blank titration, this error was estimated at 0.26M.

The pH values were determined at room temperature with a combination glass electrode, standardized at pH 2.00. Soluble iron concentrations were determined on centrifuged samples by atomic absorption spectrophotometry.

Gas Analysis

Gas analyses given in this report were obtained by denitrating 500 ml of GSWS; denitration provided gas samples representative of the instantaneous gas composition.

Gas analyses were made on a Hewlett-Packard Model 5756B gas chromatograph using a 2-m-long glass column packed with 30-60 mesh, 5A molecular sieve. The column was held at 24°C for 5 minutes before being heated at a programmed rate of 40°C/min to 300°C. The separated gases were identified by splitting the gas stream and obtaining a simultaneous mass analysis with a Finnigan Model 1015C Quadrupole Mass Spectrometer.

Denitration Tests

Initial denitration studies were conducted on nitrate-GSWS because of the complexity of the complete waste system. The sulfate and iron content of actual waste have a common origin in ferrous sulfamate used as a plutonium valence adjuster and nitrite

reductant. After the chemical processes for nitrate-GSWS denitration were defined, the more-complex chemical processes for sulfate-GSWS were prepared by substituting sulfate for nitrate; the sulfate-to-iron ratio was 2:1 to simulate actual SRP waste.

RESULTS

Experimental results of the denitrations show the equilibrium or residual concentrations of the reactants and solution properties as a function of the amount of formic acid allowed to react with 50 ml of GSWS. Evolved gas data are shown as percent nitrate reacted to form nitric oxide versus percent of the total denitration.

Nitrate-GSWS Denitrations

Residual nitrate (Figure 1) is defined by five theoretical denitration zones for the various nitrate components of the mixture. The upper zone is defined by the 0.7M nitric acid component of nitrate-GSWS. The best straight line between points A and B indicates that 2.4 ml of formic acid is sufficient to destroy the nitric acid component. The second zone is defined by the 0.35M ferric nitrate component, which appears to have been destroyed after 6.1 ml of the formic acid was added. The third zone is defined by the facile denitration of aluminum nitrate (0.35M) to

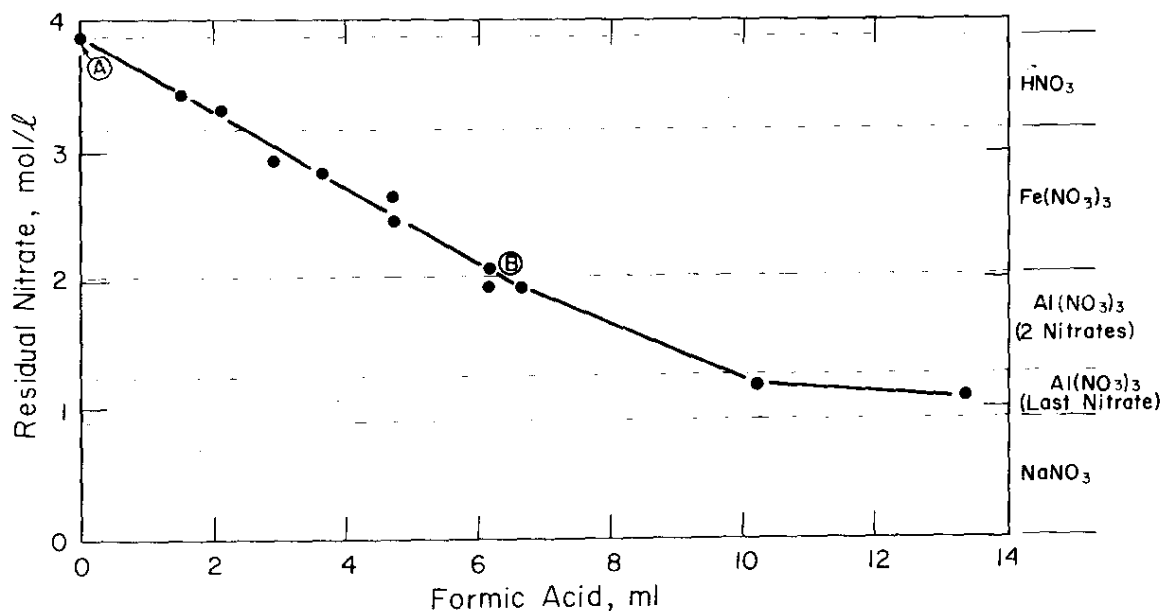


FIGURE 1. Residual Nitrate vs. Formic Acid for Nitrate-GSWS Denitration

the bis-formato complex. The fourth zone comprises the more-difficult destruction of the third nitrate associated with aluminum by formation of the tris-formato complex. The fifth zone comprises the nitrate component contributed by unreactive sodium nitrate. Equations representing the main reactions described above are given in Table 3.

TABLE 3

Reactions Involved in Denitration of Nitrate-GSWS

<i>Conditions</i>	<i>Equation for Main Reaction</i>
$\text{HNO}_3 > 4\text{M}$; HCOOH limited	$2\text{HNO}_3 + \text{HCOOH} \rightarrow \text{CO}_2 + 2\text{NO}_2 + \text{H}_2\text{O}$
$\text{HNO}_3 < 2\text{M}$; HCOOH limited	$2\text{HNO}_3 + 3\text{HCOOH} \rightarrow 3\text{CO}_2 + 2\text{NO} + 4\text{H}_2\text{O}$
$\text{HNO}_3 < 1\text{M}$; HCOOH in excess	$2\text{HNO}_3 + 4\text{HCOOH} \rightarrow 4\text{CO}_2 + \text{N}_2\text{O} + 5\text{H}_2\text{O}$
NO oxidation	$2\text{NO} + \text{O}_2 \rightarrow 2\text{NO}_2$
NO reduction	$2\text{NO}(\text{aq}) + \text{HCOOH} \rightarrow \text{N}_2\text{O} + \text{CO}_2 + \text{H}_2\text{O}$
Ferric hydrolysis and denitration	$2\text{Fe}(\text{NO}_3)_3 + 9\text{HCOOH} \rightarrow 6\text{NO} + 9\text{CO}_2 + 6\text{H}_2\text{O} + 2\text{Fe}(\text{OH})_3$
Partial aluminum complexation and denitration	$\text{Al}(\text{NO}_3)_3 + 6\text{HCOOH} \rightarrow \text{N}_2\text{O} + 4\text{CO}_2 + 5\text{H}_2\text{O} + \text{Al}(\text{HCOO})_2\text{NO}_3$
Complete denitration of aluminum by excess formic acid	$2\text{Al}(\text{NO}_3)_3 + 18\text{HCOOH} \rightarrow 3\text{N}_2\text{O} + 12\text{CO}_2 + 15\text{H}_2\text{O} + 2\text{Al}(\text{HCOO})_3$

The graph of residual formate concentrations (Figure 2) includes both free and complexed formate. Data in the region comprising the destruction of acid and ferric nitrate (Figure 1) indicate a general increase in residual formic acid. This level of residual formate is presumed to be free formic acid and not significantly associated with aluminum because about the same residual levels were found in the absence of aluminum. The data points at 10 and 13 ml formic acid show much higher levels of residual formate because of both aluminum-complexed formate and free HCOOH .

Figure 3 compares observed equivalent acidity data with the theoretical curve (ABCD). Throughout the entire range of formic acid volumes, the observed equivalent acidity is higher than the theoretical values. The origin of this difference is unknown, but similar observations have been made in SRP neutralizations with NaOH . The theoretical curve includes the 0.26M component which represents the NaOH required to adjust the diluent to pH 12. The theoretical acidity curve is composed of 3 segments. The first segment, AB, was drawn from the theoretical acidity of the synthetic waste solution with the same slope as the observed residual

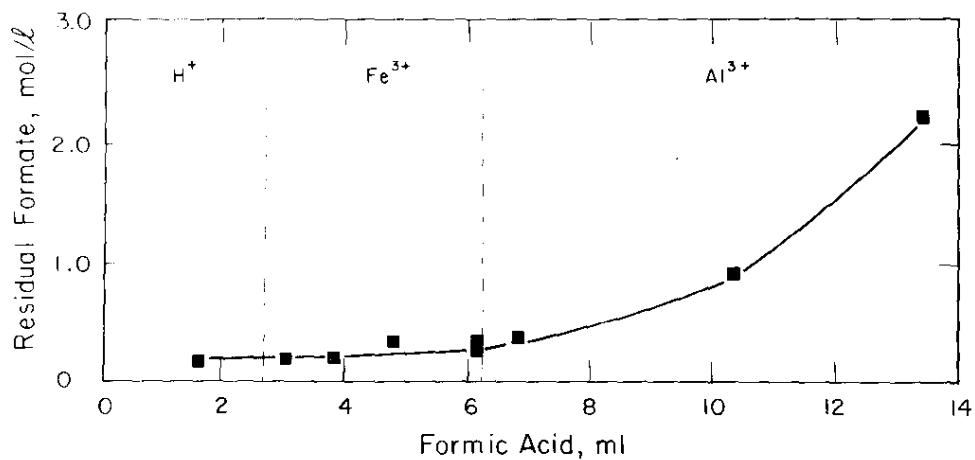


FIGURE 2. Residual Formate vs. Formic Acid for Nitrate-GSWS Denitration

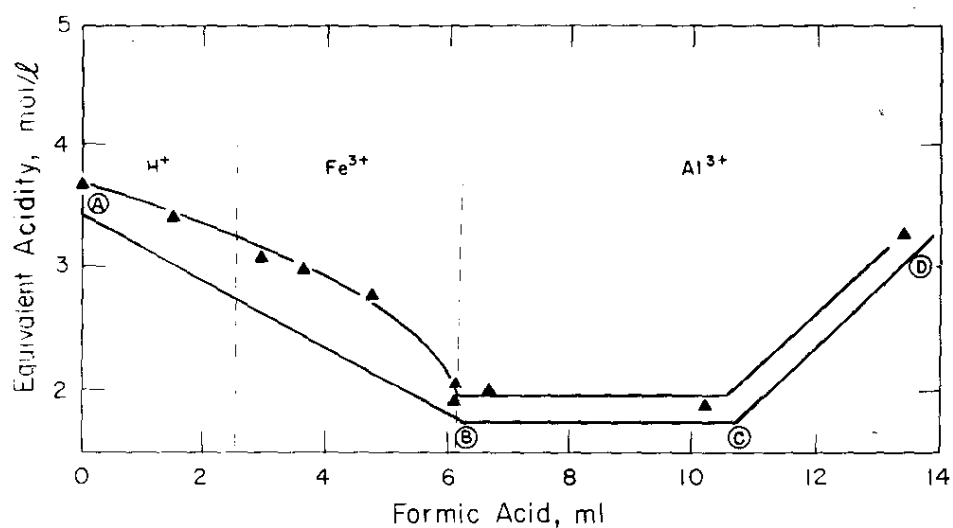


FIGURE 3. Equivalent Acidity vs. Formic Acid for Nitrate-GSWS Denitration

nitrate data (Figure 1). The segment BC is defined by the acidity of the aluminum ion compared to the aluminate ion. The last segment, CD, includes in addition to the aluminum acidity the formic acid in excess of that required for denitration and complexation.

The combination of the three graphs (Figure 4) shows internal consistency of the data and further indicates that denitration beyond destruction of hydrolyzable cations does not lower the equivalent acidity, but does increase the amount of residual formate. Eventual radiolysis of formate salts and complexes to form bicarbonate in actual waste solutions would create additional acidity and thus an additional delayed NaOH demand to maintain the desired alkalinity.

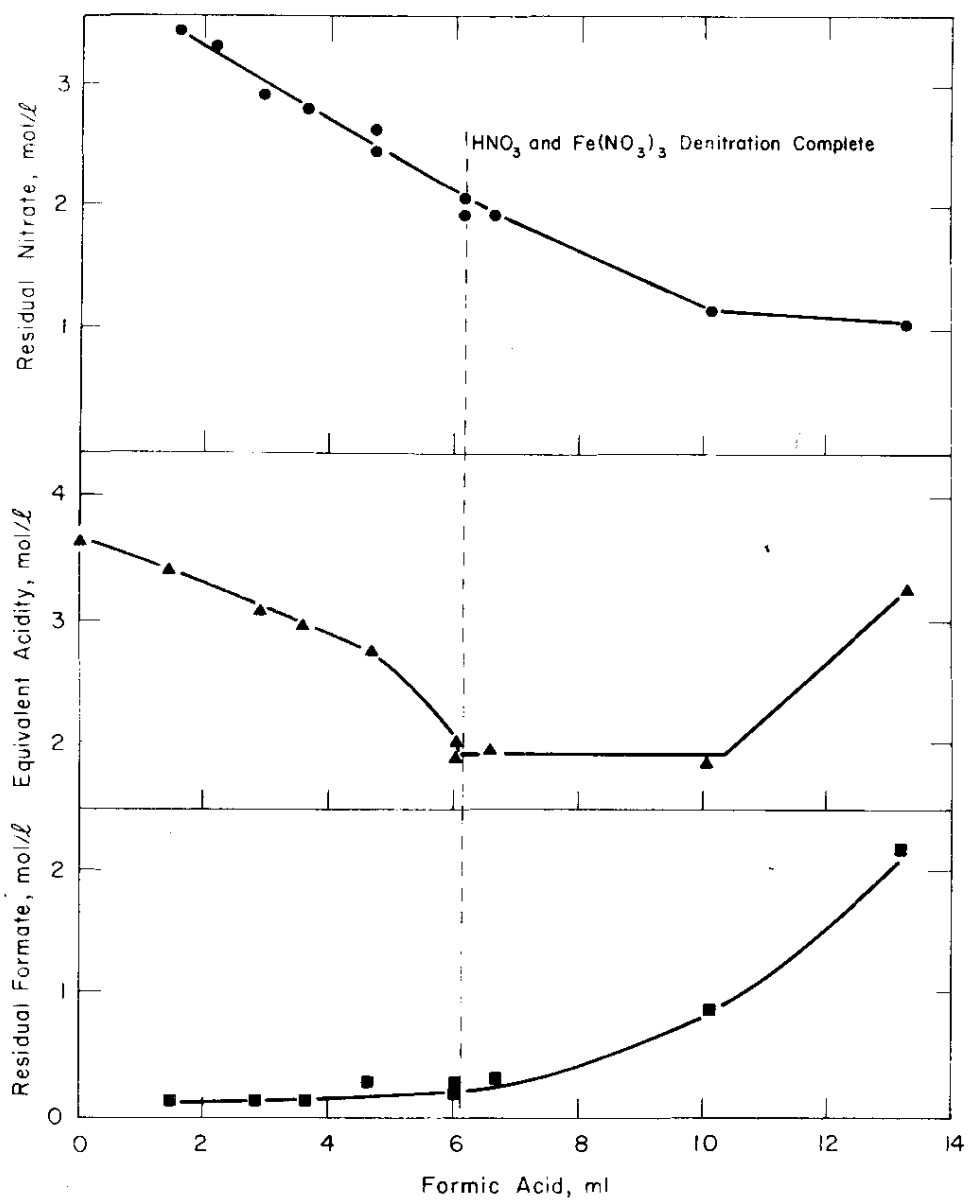


FIGURE 4. Combination of Residual Nitrate, Equivalent Acidity, and Residual Formate vs. Formic Acid

The time scale of the denitration process is illustrated by typical reaction curves such as the residual nitrate curve (Figure 5) or the evolved gas curve (Figure 6). This work suggests a minimum digestion (reflux) time of about two hours following the addition of formic acid.

Other tests demonstrated that the denitration reaction is effectively quenched by lowering the temperature to ambient when nitric acid has been reduced to $\sim 0.2M$. Completion of reaction might be detected by an NO gas analyzer.

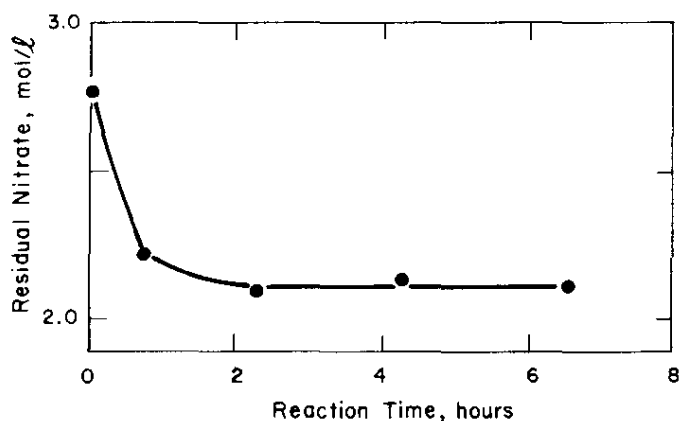


FIGURE 5. Residual Nitrate vs. Reaction Time

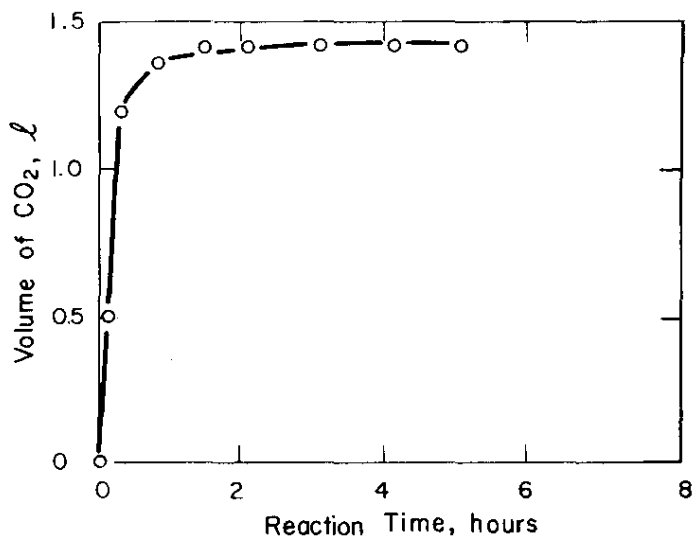


FIGURE 6. Evolved CO₂ vs Reaction Time

Several auxiliary denitration experiments were also performed to clarify other aspects of denitration. During denitration of aluminum nitrate, only the aluminum bis-formato complex was readily formed. The lanthanum tris-formato complex is readily formed in a similar denitration of lanthanum nitrate. The lanthanum complex is readily formed because of its low solubility and not because of a large stability constant. Attempts to isolate the bis-formato aluminum nitrate from solution always produced the basic formate, $\text{Al}(\text{HCOO})_2\text{OH}\cdot\text{H}_2\text{O}$, which was identified by thermogravimetric analysis and X-ray diffraction.

As mentioned earlier, the gas analysis data (Table 4 and Figure 7) were obtained for denitrations whose scale was 10 times greater than the scale used in all other tests. Figure 7 shows the effect of temperature and boilup rate on the composition of reaction products (and thus the reaction stoichiometry). The production of N_2O increased when the boilup rate was negligible.

TABLE 4

Gaseous Reaction Products in the Denitration of Nitrate-GSWS

Conditions ^a	Volume of CO_2 , λ	Percent Reaction	Gas Composition, %		
			NO	N_2O	CO_2
Under reflux at $\sim 103^\circ\text{C}$	2.0	4.8	35.1	3.7	64.2
	6.0	14.6	35.8	4.5	61.8
	13.5	32.8	30.2	7.8	66.0
	25.0	60.8	19.8	12.0	72.2
	35.0	85.2	25.5	10.0	67.0
	41.1	100	36.2	4.8	57.7
Negligible reflux at 100°C	2.0	4.8	33.0	4.0	60.0
	6.0	14.5	32.0	6.8	64.8
	13.5	32.6	23.3	10.7	67.8
	25.0	60.3	12.4	14.2	67.8
	34.5	83.2	13.0	14.4	70.3
	41.4	100	12.6	16.8	74.9
Negligible reflux at 80°C	2.0	4.8	21.2	6.2	76.5
	6.0	14.5	25.2	8.5	63.2
	13.5	32.5	16.7	14.0	72.0
	25.0	60.6	3.1	18.7	75.8
	33.6	80.0	2.8	20.2	81.0
	36.0	87.2	3.8	20.0	81.2

a. 500 ml of GSWS reacted with 51.2 ml of 24M formic acid, which is sufficient to destroy both free HNO_3 and $\text{Fe}(\text{NO}_3)_3$ at a reactant ratio of 1.5.

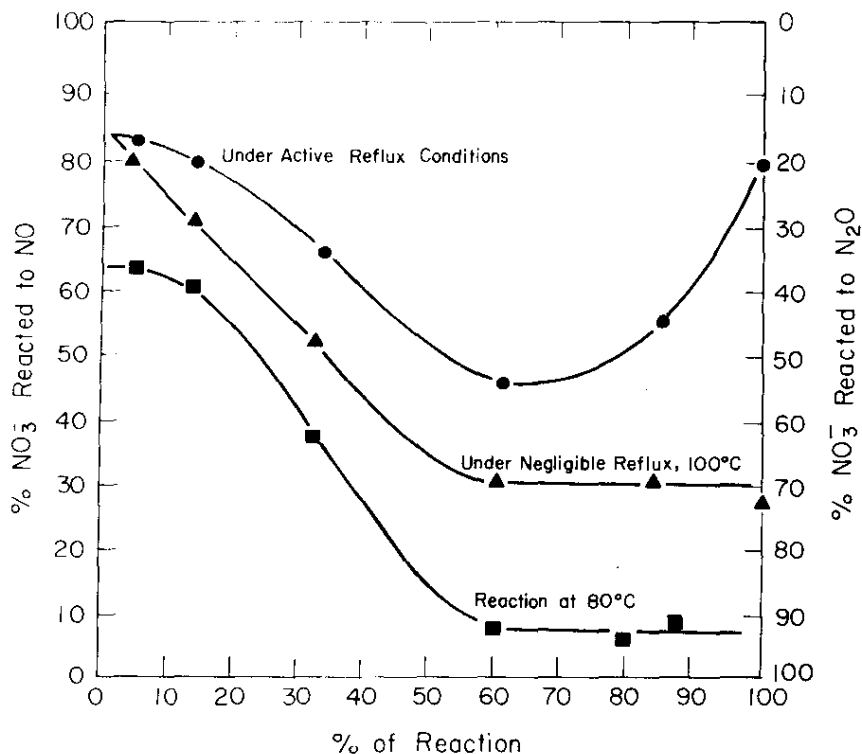


FIGURE 7. Variation of NO/N₂O Production During Denitration

The increase in NO production under active boilup conditions is believed to result from an irreversible hydrolysis of ferric nitrate occurring under these conditions. Higher reaction rates, combined with the stripping action of steam evolution, decrease the mean residence time of NO in solution and hence decrease its chance of reduction to N₂O.

The effect of temperature on the reaction products is illustrated in the lowest curve in Figure 7, which shows that a lower reaction temperature also enhances N₂O production. The lower temperature increased the normally insignificant (2 to 3 min) induction period to about 20 minutes, and the overall reaction rate was decreased. Because of this decrease the reaction was only 87% complete in the 6 hours normally allocated for the denitrations.

The induction period for denitrations is a previously observed phenomenon whose origin has been attributed to reaching

a threshold concentration of nitrous acid.^{4,5,7} The time required to attain this threshold concentration is a function of acidity, temperature, and initial nitrite concentration. For denitration at 80°C, the constant addition of formic acid was stopped after the addition of 8 ml (equivalent to 0.4M formic acid) to allow the reaction to start. After about 3 to 4 l of gas was evolved, addition of formic acid was continued at the normal rate of 2.5 ml/(min-l) as recommended by Bradley, et al.,⁵ for large-scale denitrations.

Sulfate-GSWS Denitrations

After denitrations of nitrate-GSWS were completed, the denitration of the more-complex sulfate-GSWS was studied. Before the denitration tests, the ionic composition of the untreated stock solution was established. Although this solution was made up by the combination of sodium bisulfate and the nitrates of iron, aluminum, and sodium, the sulfate was immediately complexed by iron and aluminum. The protons originally complexed by sulfate were displaced and thereby contributed to the free acidity of the solution. The observed pH (~ 0.05) corresponded to a free acidity of 0.72M when compared to a calibration curve established for the solution's ionic strength of 2.4M. This ~ 0.7 M free acidity indicated that not only was sulfate complexed, but ferric sulfate was not significantly hydrolyzed at this acidity. Additional tests showed that the ferric sulfate complex was partially hydrolyzed at acidities of 0.4M, whereas the aluminum sulfate complex was not. Thus, the original stock solution is most accurately described as: 0.7M HNO_3 , 0.35M FeSO_4NO_3 , 0.35M AlSO_4NO_3 , and 1.0M NaNO_3 .

The sequence of denitration for sulfate-GSWS is indicated on the residual nitrate graph (Figure 8). Table 5 shows equations

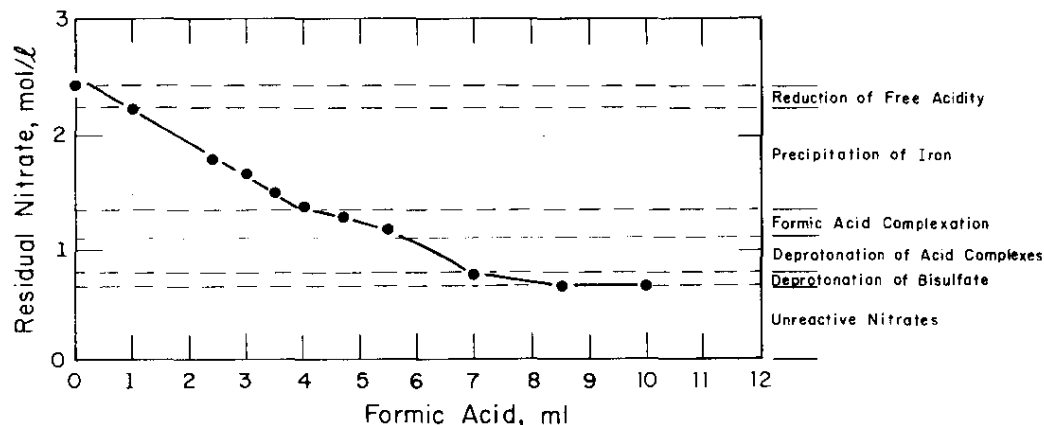


FIGURE 8. Residual Nitrate vs. Formic Acid for Sulfate-GSWS Denitration

for the reactions referenced in the text. The first region in Figure 8 corresponds to destruction of free acid to the point that hydrolysis of ferric ion becomes significant. The second region includes all denitrations which coincide with hydrolysis and precipitation of the ferric component of the solution. The third region consists of all denitrations which coincide with addition of formic acid to the aluminum sulfate species to form the mixed complex $[Al(SO_4) \cdot HCOOH]^+$. The fourth region includes denitrations which coincide with deprotonation of the mixed complex previously formed. The fifth region is attributed to denitration promoted by protons from bisulfate species.

TABLE 5

Equations of Reactions Involved in the Denitration of Sulfate-GSWS

1. $2HNO_3 + HCOOH \rightarrow 2NO + 3CO_2 + 4H_2O$
2. $2HNO_3 + 4HCOOH \rightarrow N_2O + 4CO_2 + 5H_2O$
3. $Fe(SO_4)NO_3 + H_2O \rightleftharpoons Fe(SO_4)(OH) + HNO_3$
4. $Fe(SO_4)(OH) + H_2O + NaNO_3 \rightleftharpoons NaFe(SO_4)(OH)_2 + HNO_3$
5. $3NaFe(SO_4)(OH)_2 \rightarrow NaFe_3(OH)_6(SO_4)_2 + Na_2SO_4$
6. $3FeSO_4^+ + 4NO_3^- + 6H_2O + Na^+ \rightarrow Na[Fe(OH)_2]_3(SO_4)_2 + 5H^+ + 4NO_3^- + HSO_4^-$
7. $Al(SO_4)^+ + NO_3^- + HCOOH \rightarrow [Al(SO_4) \cdot HCOOH]^+ + NO_3^-$
8. $[Al(SO_4) \cdot HCOOH]^+ + NO_3^- \rightarrow [Al(SO_4)(HCOO)] + H^+ + NO_3^-$

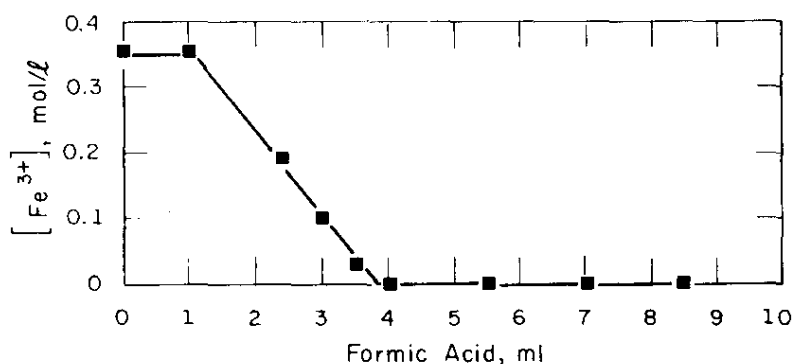


FIGURE 9. Residual Soluble Iron vs. Formic Acid for Sulfate-GSWS Denitration

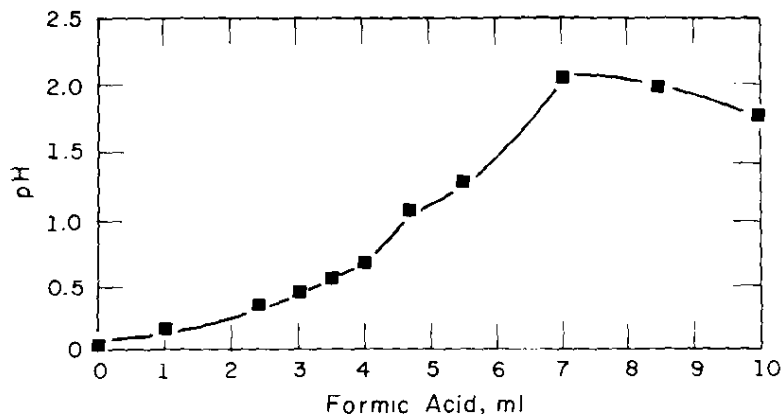


FIGURE 10. Equilibrium pH vs. Formic Acid for Sulfate-GSWS Denitration

The residual iron data in Figure 9 show that hydrolysis and precipitation of iron occurred only after a minimum of 1.0 ml of formic acid was allowed to react with sulfate-GSWS. As shown from the pH of the equilibrium mixture (Figure 10) at 1 ml of formic acid and the calibration curve for free acidity at 2.4M ionic strength, hydrolysis of the ferric sulfate complex did not begin until the free acidity was reduced to about 0.5M. Thus, the free acidity of any sulfate system must be reduced to about 0.5M before hydrolysis can occur. The main reaction occurring in this region is given in Equation 1 (Table 5); Equation 2 is a secondary reaction. Throughout the entire denitration, the average reaction changes with increasing pH from Equation 1 to Equation 2.

The second denitration region in Figure 8 includes several reactions in addition to those given for the actual destruction on nitric acid by formic acid. The equilibrium pH data show that after the reaction of 4 ml of formic acid, which corresponds to complete precipitation of ferric ion, the free acidity was reduced to ~0.2M. Thus, more protons were consumed by denitration reactions than were liberated by hydrolysis and precipitation of the ferric component. [Iron was precipitated as sodium jarosite, $\text{NaFe}_3(\text{OH})_6(\text{SO}_4)_2$, which was identified by both x-ray diffraction and chemical analysis.]

The continuous precipitation of sodium jarosite (i.e., the linear decrease in soluble iron) indicates a pH control of the first hydrolysis reaction, Equation 3, of the aqueous ferric sulfate complex. The second hydrolysis, Equation 4, appears to coincide with the first, leading to the formation of sodium jarosite (Equation 5). Thus, the complete precipitation of iron is driven by an increasing pH of the reaction solution according to the overall reaction given by Equation 6.

The acidity of the system was decreased by two mechanisms:

- 1) the simple destruction of nitric acid by formic acid, and
- 2) the complexation of protons by sulfate liberated by the precipitation of jarosite. The second mechanism was unique to this GSWS and other solutions in which there is not an excess of cations which would form more-stable sulfate complexes than would the acidic protons. Thus, the proton inventory of the solution was $\sim 0.1\text{M}$ higher than that indicated by the pH. This allows a reasonable material balance between the 0.9M nitrate destroyed in the second region, the sum of the protons released by hydrolysis (0.7M), the decrease in solution acidity (0.3M), and the formation of acid sulfate (-0.1M).

The proposed addition of molecular formic acid to the aluminum sulfate complex as given in Equation 7 (Table 5) is based on the experimental data over the range of 4.0 to 5.5 ml of added formic acid. The nitrate data (Figure 8) and the equilibrium pH data (Figure 10) indicate that 0.2M free nitric acid was destroyed in this region. Thus, from the reaction stoichiometry and the incremental addition of formic acid, residual formate should increase by $\sim 0.4\text{M}$; and the residual formate curve (Figure 11) shows that just this amount was observed. The ratio of this increase in residual formic acid to the aluminum sulfate complex is about 1:1. This correlation is the basis for the proposed addition reaction (Equation 7). The equivalent acidity data (Figure 12) also show the expected increase in acidity in this region. Similarly the evolved carbon dioxide curve (Figure 13) shows that less formic acid is being reacted to CO_2 than is being introduced.

Deprotonation of the acid complex (Equation 8) is supported by the residual formate curve which shows that no additional unreactive formate appeared in the equilibrium mixture as a consequence of the reactions in this region. Because the available free acidity was very small throughout the region and formic acid

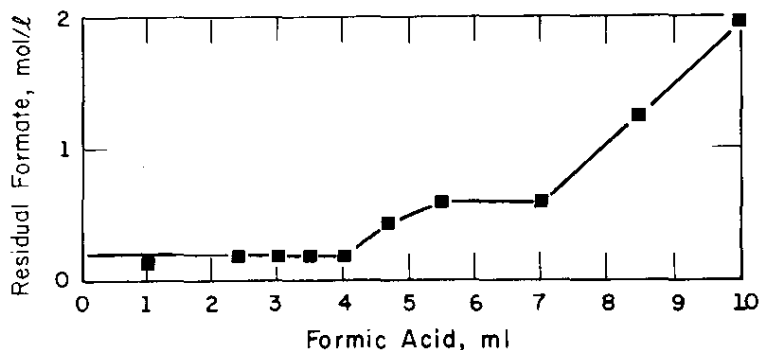


FIGURE 11. Residual Formate vs. Formic Acid for Sulfate-GSWS Denitration

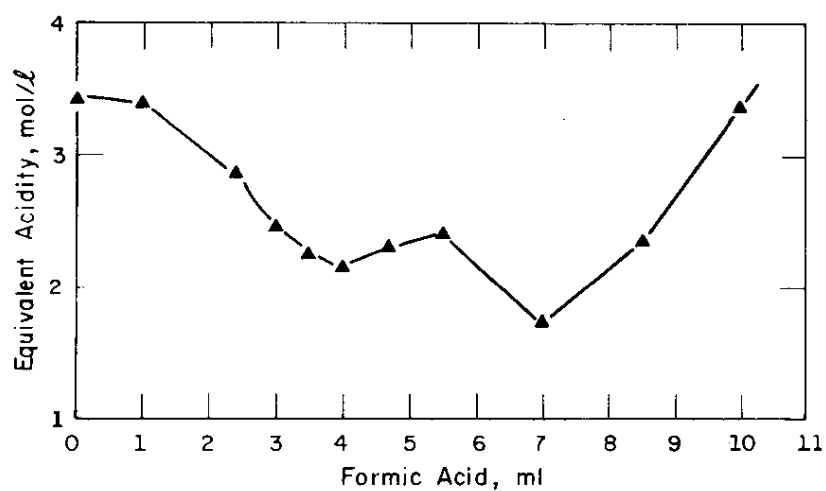


FIGURE 12. Equivalent Acidity vs. Formic Acid for Sulfate-GSWS Denitration

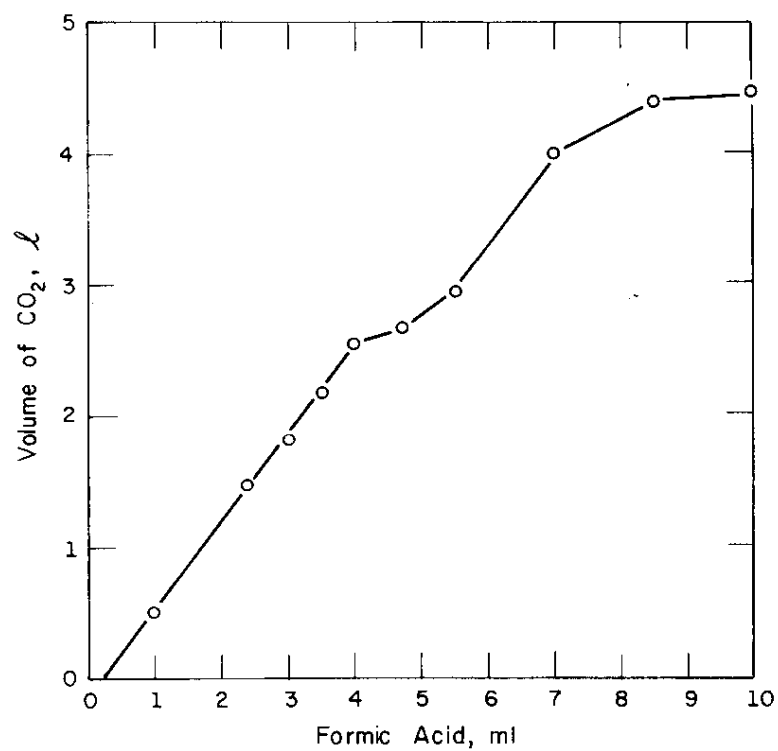


FIGURE 13. Evolved Carbon Dioxide vs. Formic Acid for Sulfate-GSWS Denitration

itself can not drive denitration, the proton source must be a more acidic species, i.e., the acid complex. The equivalent acidity curve also reflects the deprotonation of the acid complex. Moreover, the excess equivalent acidity (as compared to theoretical calculations) is eliminated in this region. No explanation of this excess acidity has been found consistent with the total data set.

Denitration of the sulfate-GSWS is fundamentally different from the nitrate-GSWS since the denitration proceeds only to the destruction of two moles of nitrate per mole of ferric and one mole of nitrate per mole of aluminum.

Denitration of Simulated Purex LAW

Although the gases evolved in the denitration of sulfate-GSWS were not analyzed, those evolved during denitration of a simulated Purex LAW (see Table 1) at 105°C and active reflux were analyzed. These data are shown in Figure 14 and were interpreted on the basis of the reaction sequences described for the sulfate-GSWS. Thus, the initial reaction was the simple reduction of free acidity to ~0.5M with more than 70% of the nitrate reacted being reduced to NO. The second stage involved hydrolysis of

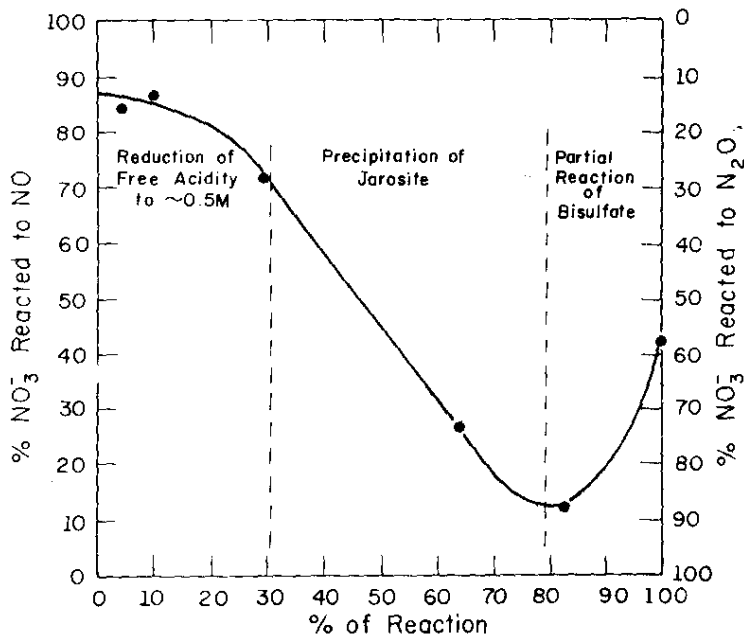


FIGURE 14. Variation of NO/N₂O Production During Partial Denitration of a Simulated Purex-LAW Solution (Under Active Reflux with Sulfur Buffering)

the ferric sulfate complex and its precipitation as sodium jarosite, which was driven by a reduction in free acidity to ~0.2M. Also, the reaction products changed dramatically toward the predominant production of N₂O. In the final stage, bisulfate acted as a proton source for the remaining denitration. This denitration was not carried to completion, due to the limited amount of formic acid added. The apparent increase in NO production in this final stage when the system is under active reflux cannot be explained at this time.

An identical denitration test at 100°C did not show this final increase in NO production. However, the lower reaction temperature was found to inhibit precipitation of jarosite without affecting the extent of denitration. Denitration at less than reflux temperatures was not pursued further.

Reaction Mechanisms

In this section, possible mechanisms which explain the reaction products observed in denitrations with formic acid are proposed. Although this study did not produce kinetic data, observations concerning the production of various oxides of nitrogen under known conditions provided additional information by which mechanisms could be proposed. The kinetics were studied by Longstaff and Singer,⁷ who proposed many of the free radical reactions given in Table 6. However, their study was incomplete

TABLE 6
Equations of Reaction Mechanisms

HNO₂-Formation Reactions

- (1) $2\text{NO}_2 + \text{H}_2\text{O} \rightarrow \text{HNO}_2 + \text{HNO}_3$
- (2) $\text{NO}_2 + \text{HNO}^* \rightarrow \text{HNO}_2 + \text{NO}$
- (3) $\text{HNO}_3 + \text{HCO}_2^* \rightarrow \text{HNO}_2 + \text{CO}_2 + \text{OH}^*$
- (4) $\text{HNO}_3 + \text{HNO}^* \rightarrow 2\text{HNO}_2$

HNO₂-Destruction Reactions

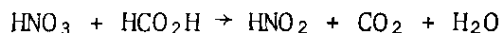
- (5) $\text{HNO}_2 + \text{HCO}_2\text{H} \rightarrow \text{HNO}^* + \text{CO}_2 + \text{H}_2\text{O}$
- (6) $\text{HNO}_2 + \text{HNO}_3 \rightarrow 2\text{NO}_2 + \text{H}_2\text{O}$
- (7) $\text{HNO}_2 + \text{HCO}_2\text{H} \rightarrow \text{NO} + \text{HCO}_2^* + \text{H}_2\text{O}$
- (8) $\text{HNO}_2 + \text{HCO}_2^* \rightarrow \text{NO} + \text{CO}_2 + \text{H}_2\text{O}$

HNO-Destruction Reactions*

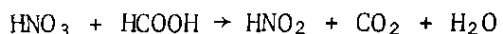
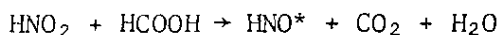
- (9) $\text{HNO}^* + \text{NO} \rightarrow \text{N}_2\text{O} + \text{OH}^*$
- (10) $\text{HNO}^* + \text{HNO}^* \rightarrow \text{N}_2\text{O} + \text{H}_2\text{O}$
- (11) $\text{HNO}^* + \text{HNO}^* \rightarrow \text{N}_2 + 2\text{OH}^* (\text{H}_2\text{O}_2)$

in that they based their conclusions only on nitrite analysis and volumetric gas analyses for CO_2 . The existence of nitrous oxide as a reaction product was not recognized in previous work due to incomplete characterization of the reaction products. Healy's study⁴ of denitration with formaldehyde and formic acid also did not recognize the formation of nitrous oxide as a reaction product, although it probably was formed under his experimental conditions. Healy's work did show that the reaction mechanism for denitration with formaldehyde is quite different from that of formic acid because of the greater reducing power of formaldehyde.

Previous studies⁷ established that nitrous acid (HNO_2) is an essential intermediate in the denitration scheme. Because HNO_2 is destroyed by various reactions, this species must be continuously regenerated. Of the first four reactions given in Table 6, only the hydration of nitrogen dioxide (Equation 1) does not involve radical intermediates. However, under high acid conditions, the equilibrium lies far to the left, which does not suggest a prominent role for this mechanism under high acid conditions. Nitrous acid formation via reaction of the HNO radical and NO_2 (Equation 2) does not proceed in high acid conditions since the reaction produces nitric oxide (NO), which is not a major product at high acid concentrations. This leaves two possible high-acidity reactions (Equations 3 and 4) of molecular nitric acid with radical intermediates. The overall production of nitrous acid via the formate radical can be represented by the following:



whereas the same overall reaction with the HNO^* radical can be represented by:



Formation of nitrous acid via the HNO radical is important because this radical appears to be the only feasible intermediate for production of nitrous oxide (N_2O). However, because the production of this radical depends on a bi-molecular reaction, nitrous acid production via the formate-hydroxy radical cycle is probably much more important under conditions of low formic acid concentration and high acidity.

Reactions leading to the destruction of HNO_2 can also be ranked in order of probable importance under differing acidities. The importance of the direct reaction with formic acid (Equation 5) to form the essential radical intermediate, HNO^* , in N_2O formation was mentioned. Though nitrous acid functions as an oxidant under moderate to low acidities, it can be oxidized to NO_2 by strong nitric acid (Equation 6). High acidity also reduces the formation of the HNO^* (Equation 5) radical and accounts for the lack of N_2O observed in the reaction products. This suggests that, at low formic acid concentration and high acidity, the formate radical cycle is predominant in maintaining HNO_2 production. Support for this argument was found in Longstaff and Singer's study,⁷ which showed that the second order rate constant increased rapidly up to 12.5M and then decreased between 12.5 and 18.4M nitric acid. Thus, under reaction conditions in which formic acid is reacting to form nitrous acid at a rate equal to its addition rate, the main reaction product is expected to be NO_2 .

In practice, denitration cannot be carried out under conditions such that the addition rate of formic acid is equal to the reaction rate. Thus, a constant addition rate of formic acid eventually becomes greater than the reaction rate leading to NO_2 , whereupon the formic acid concentration increases, and the direct reaction (Equation 7) of nitrous and formic acids occurs to form NO . The formate radical can react with more nitrous acid as in Equation 8, or more likely react to form more nitrous acid as in Equation 3. The main reaction products gradually shift from NO_2 to NO during a denitration with a constant addition rate of formic acid. Another result of the increasing formic acid concentration is the increasing production of nitrous acid via the HNO radical.

The decreasing acidity and concurrent increasing formic acid concentration promote formation of nitrous oxide via Equations 9 and 10. However, di-radical reactions are statistically improbable so that Equation 9 is believed to be the main reaction producing N_2O . Because Equation 9 involves nitric oxide, whose solubility is limited in the reaction mixture, the formation of N_2O would probably be dependent on factors which influence the concentration of NO in the reaction mixture. This was observed to occur for various reaction parameters. Reduced N_2O production was observed with increased boilup rate with the reaction under reflux. The increased steam generation increased the transport of NO out of solution and into the gas phase. Conditions which reduce the formation rate of NO (Equation 7) by the bi-molecular reaction would increase its average residence time in solution and hence the probability of reaction via Equation 9. Such conditions were shown to include reaction temperature and acidity buffered so as to reduce the reactivity. At lower reaction

temperature and buffered hydrogen ion activity, 100% conversion to N_2O was observed in contrast to about 50% under normal conditions.

Equation 11 (Table 6) represent a possible mechanism for production of nitrogen as a reaction product. This mechanism would be of low probability under the best conditions, and thus is not believed to be the source of the almost constant amount of nitrogen detected in the reaction gases. This nitrogen is believed to be introduced during the sampling procedure for gas chromatographic analysis.

REFERENCES

1. L. A. Bray. *Denitration of Purex Wastes with Sugar*. USAEC Report HW-76973 REV, Hanford Atomic Products Operation, Richland, WA (1963).
2. R. C. Forsmon and G. C. Oberg. *Formaldehyde Treatment of Purex Radioactive Wastes*. USAEC Report HW-79622, Hanford Atomic Products Operation, Richland, WA (1963).
3. T. V. Healy. "The Reaction of Nitric Acid with Formaldehyde and with Formic Acid and Its Application to the Removal of Nitric Acid from Mixtures." *J. Appl. Chem.* 8, 553 (1958).
4. W. H. Adams, E. B. Fowler, and C. W. Christenson. "A Method for Treating Radioactive Nitric Acid Wastes Using Paraformaldehyde." *Ind. Eng. Chem.* 52 (1), 55 (1960).
5. R. F. Bradley and C. B. Goodlett. *Denitration of Nitric Acid Solutions by Formic Acid*. USAEC Report DP-1299, Savannah River Laboratory, E. I. du Pont de Nemours and Company, Aiken, SC (1972).
6. H. Krause and R. Randl. *Treatment and Final Disposal of Radioactive Wastes from Fuel Reprocessing in the Federal Republic of Germany*. German Report KFK-1741, Gesellschaft für Kernforschung M.B.H., Karlsruhe, Germany (19).
7. J.V.L. Longstaff and K. Singer. "The Kinetics of Oxidation by Nitrous Acid and Nitric Acid. Part II. Oxidation of Formic Acid in Aqueous Nitric Acid." *J. Chem. Soc.* 1954, 2610 (1954).